
Heller, Valentin (2017) Scale effects in shallow-water vortices. In: 4th International Symposium on Shallow Flows (4th ISSF), 26-28 June 2017, Eindhoven, Netherlands.

# Scale effects in shallow-water vortices

V. Heller[1]

[1] Geohazards and Earth Processes Research Group, Faculty of Engineering, University of Nottingham, Nottingham NG7 2RD, UK
Email: Valentin.heller@nottingham.ac.uk

*Keywords: physical modelling, Reynolds number invariance, scale effects, scale series, shallow-water vortices.*

**Abstract**

A widely applied model strategy in experimental fluid dynamics is to conduct laboratory experiments at reduced scale in the Reynolds number R invariant regime to ensure that the turbulent behaviour in the field situation is correctly modelled. This study investigates R invariance and quantifies R scale effects in dissipative-type shallow-water vortices where R invariance can naturally not be maintained. A laboratory scale series of monopole shallow-water vortices was conducted in a circular domain with rotating bottomless cylinders. Froude scale ratios were applied to carefully scale all experimental parameters between three scales, apart from the kinematic viscosity. Surface particle image velocimetry was conducted to record the vortex decay. The radial-averaged azimuthal velocity over radial distance and the ensemble-averaged mean azimuthal velocity, Reynolds number and dimensionless vorticity decays are presented. A similar pattern in the initial turbulent regime is observed in all three scales for the vorticity whilst the decays deviate in the transition and laminar regime. Such results help to quantify scale effects and to improve the modelling of shallow-water vortices in Froude models. The results reveal several interesting research questions which will be addressed in the near future.

## 1. Introduction

A widely applied model strategy in experimental fluid dynamics is to conduct laboratory experiments at reduced scale at sufficiently high Reynolds number R, in the R invariant regime, to ensure that the turbulent behaviour in the field situation is correctly modelled and significant scale effects are excluded (Heller, 2011; 2017). This study investigates R invariance and quantifies R scale effects in dissipative-type shallow-water vortices where R invariance can naturally not be maintained over the entire vortex evolution. Coriolis effects are thereby not considered. Shallow-water vortices in this context are relevant in many engineering and small-scale geographical contexts such as vortex shedding behind groynes in rivers, landslide-tsunami generation, vortices at intakes, wave energy converters in the coastal region and tidal efflux eddies from coastal lagoons (Jirka, 2001). This work particularly focuses on vortices observed in Froude models, where a primary phenomenon (water waves, open channel flows, etc.) is governed by gravity and inertial forces. Vortices, as secondary phenomenon, are then also forced into Froude scaling, which is a poor model for inertia and viscosity dominated vortices. The overall aims of this study are (i) to provide a better physical understanding of dissipative-type shallow-water vortices, (ii) to reveal the conditions under which R invariance is achieved for vortices and (iii) to quantify scale effects observed in a later phase of the vortex evolution where R invariance does not apply.

## 2. Physical model

Laboratory experiments have been conducted in a 1.80 m long, 1.01 m wide and 0.34 m deep water tank as shown in Fig. 1. The shallow-water vortices were generated with rotating bottomless cylinders, actuated with a DC motor. The cylinders rested on a supporting structure allowing for a small gap between the cylinders and the bottom of the water tank. The cylinder rotation and its vertical removal after spin-up were controlled via LabView®. The cylinders were then manually shifted sideward to carry out surface Particle Image Velocimetry (PIV). The spin-up time was large enough to actuate the entire fluid body within the circular boundary such that the fluid decayed as a monopole vortex.

A Froude scale series consisting of three scales (1:$\lambda$ = 1:1, 1:2 and 1:4 with $\lambda$ = a characteristic length in the largest scale/corresponding length in smaller scale) has been conducted. The scale series involved three water depths ($h$ = 0.08, 0.04, 0.02 m), outside diameters of inner cylinders ($2r_i$ = 0.300, 0.150, 0.075 m), inner diameters of outer cylinders ($2r_o$ = 1.000, 0.500, 0.250 m), cylinder wall thicknesses (0.0060, 0.0030, 0.0015 m), ramp-up times (8.0, 5.7, 4.0 s), spin-up times (60.0, 42.4, 30.0 s) and initial angular velocities ($\Omega_0$ = 12.57, 17.77, 25.13 rad/s) (Fig. 1b,c). The ramp-up time is the time required for a cylinder to reach the initial angular velocity. The initial Froude number was $v_0/(gh)^{1/2}$ = 2.13 and the initial Reynolds numbers were $v_0h/\nu$ = 172,586, 60,718 and 20,826, with the azimuthal velocities $v_0 = \Omega_0 r_i$ (1.89, 1.33, 0.94 m/s), kinematic viscosities $\nu \approx 0.9 \cdot 10^{-6}$ m²/s and gravitational acceleration $g$. The shallowness parameter $S = 2r_i/h$

= 3.75 was selected to ensure quasi two-dimensional flow conditions given by $S > 3.0$ in combination with a sufficient large R (Seol and Jirka, 2010). PIV was conducted for 120.0, 84.9 and 60.0 s, at sampling rates of 15.0, 21.2, 30.0 Hz, over analysed PIV areas of $\Delta x \times \Delta y = 0.516 \times 0.516$, $0.258 \times 0.258$ and $0.129 \times 0.129$ m$^2$ and with interrogation window sizes of $4 \times 4$, $2 \times 2$ and $1 \times 1$ mm$^2$ from large to small scale, respectively. Several further parameters were carefully scaled including the gap size between cylinder and tank bottom (to avoid friction effects) and the seeding particle diameter. All results represent ensemble averages of 3-4 runs.

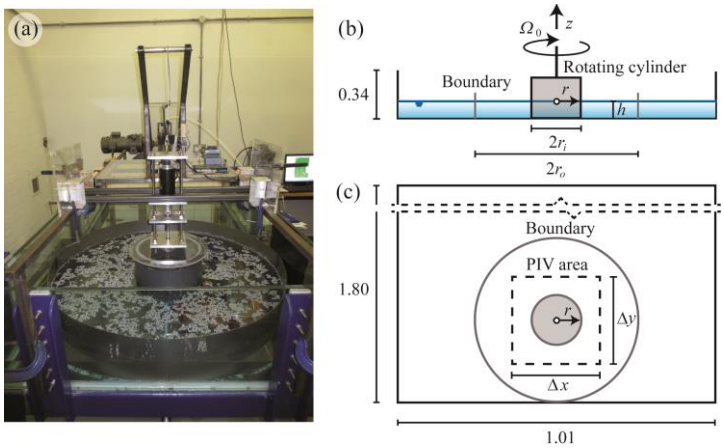


Figure 1: (a) picture of set-up at $\lambda = 1$ prior to start of experiment, (b) side view of cylinder at $\lambda = 2$ with main parameters and (c) plane view at $\lambda = 2$ with PIV area.

## 3. Results

### 3.1 Velocity distribution

Figure 2 shows the radial-averaged azimuthal velocity $v$ over the radial distance $r$ for all three scales. Note that the width of the PIV area covers only 52% of $2r_o$ (Fig. 1c). The data is shown at 20, 40, 80 and 120 s at the largest scale and for the corresponding scaled moments in times for $\lambda = 2$ and 4. The velocity does not always reach exactly zero at the vortex centre location due to its unsteadiness. The maximum velocity in Fig. 2a is $v(t = 20\text{ s}; r \approx 0.11\text{ m}) \approx 0.17$ m/s which is only about 9% of the initial azimuthal velocity of $\Omega_0 r_i = 1.89$ m/s, i.e. the fluid rotates significantly more slowly than the cylinders. The velocity profiles decrease with time and become smoother. The maximum velocity in Fig. 2b is $v(t = 14.1\text{ s}; r \approx 0.13\text{ m}) \approx 0.11$ m/s and $v(t = 10\text{ s}; r \approx 0.066\text{ m}) \approx 0.063$ m/s in Fig. 2c, and tends to move further towards the peripheries with decreasing scale. The smaller the scale, the faster solid body rotation (given by an azimuthal velocity $u = \omega r$) is approached. These velocity values within the PIV area are slightly smaller than after Froude scaling which would result in $v\lambda^{-1/2} = 0.17/2^{1/2} = 0.120$ m/s for $\lambda = 2$ and $0.17/4^{1/2} = 0.085$ m/s for $\lambda = 4$. The fluid at $\lambda = 2$ and 4 behaves more viscous in relation to the largest scale as the kinematic viscosity is not scaled. The fluid thus takes on less vorticity from the cylinders during spin-up and the vortices decay relatively faster with decreasing scale.

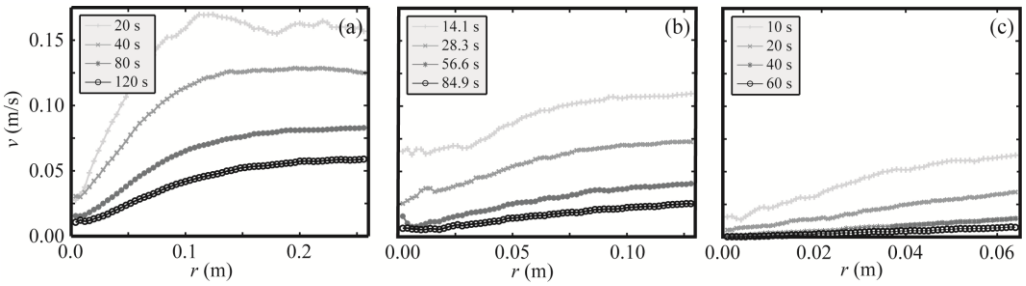


Figure 2: Radial-averaged azimuthal velocity $v$ over radial distance $r$ for different moments in time for (a) $\lambda = 1$, (b) $\lambda = 2$ and (c) $\lambda = 4$.

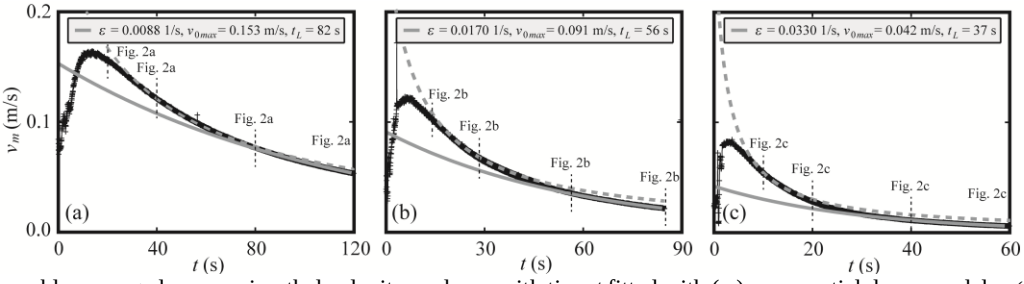


Figure 3: Ensemble-averaged mean azimuthal velocity $v_m$ decay with time $t$ fitted with (—) exponential decay model $v_m(t) = v_{0max} \cdot \exp(-\varepsilon t)$ and (- -) power curves; the transition time $t_L$ corresponds to the time when the exponential decay model deviates from the data.

Figure 3 shows the mean (over PIV area) velocity $v_m$ decay with time for all three scales. The velocities in all scales follow the same trend; the data increases in the initial stage, reaches a peak and then starts to decay due to bottom and side wall friction. The occurrence of these peaks seems to be associated with the reformation of the shallow-water vortices in the initial stage of the experiments as well as the PIV seeding redistribution and surface wave decay caused by the cylinder removal. The peak values are 0.164 m/s (Fig. 3a), 0.123 m/s (Fig. 3b) and 0.083 m/s (Fig. 3c) which are 100·0.164/1.89 = 8.7%, 100·0.123/1.33 = 9.2% and 100·0.083/0.94 = 8.8% of the corresponding initial azimuthal velocities $\Omega_0 r_i$. The magnitudes of these peaks in the smaller scales follow Froude scaling $\lambda^{1/2}$ in relation to the largest scale whilst the timing of the peaks (13.7, 6.5, 3.0 s) decreases significantly faster than after Froude $\lambda^{1/2}$ due to currently unknown reasons. The exponential and power curves in Fig. 3 are addressed in the next section.

### 3.2 Critical Reynolds number and vorticity

An important question for the present work is when the transition between turbulent (R invariance) and transition or laminar flow occurs, i.e. under which conditions scale effects become significant. Figure 4a shows $v_m(t)h/\nu$ over time $t$ for all three scales. The shapes of the curves follow the same trend as the velocity in Fig. 3. The critical R criteria for open channel flow $vh_R/\nu \approx vh/\nu = 1000$ ($h_R$ = hydraulic radius) to distinguish between fully turbulent and transitional flow and 575 between transitional and laminar flow are also included in Fig. 4a. However, an alternative criterion needs to be found for the present application as another characteristic velocity is used.

An alternative method to identify a critical R may be to define the transition time scale with the velocity decay. The decay due to viscous dissipation follows $t^{-1}$ in the turbulent and $\exp(-t)$ in the laminar regime (Seol and Jirka, 2010). An exponential decay model may thus be applied to the data of the present study with $v_m(t) = v_{0max}\exp(-\varepsilon t)$ where $\varepsilon$ is a scale specific constant decay rate and $v_{0max}$ is an initial interpolated maximum azimuthal velocity. This model may reveal a time scale for the laminar regime and power curves may help to identify the transition time scale of the turbulent regime.

The solid grey lines in Fig. 3 represent the exponential decay found with curve fitting with the decay rates $\varepsilon$ shown in the legends. The transition time scale $t_L$ can be defined as the moment in time when the exponential decay deviates from the data. The times $t_L$ = 82, 56 and 37 s follow Froude scaling $\lambda^{1/2}$ whilst $\varepsilon$ = 0.0088, 0.0170 and 0.0330 $s^{-1}$ follow $\lambda^{-1}$, which differs from both Froude scaling $\lambda^{-1/2}$ and Reynolds scaling $\lambda^{-2}$. The transition R identified with this decay model are 6874, 1621 and 277 (Fig. 4a) such that they vary up to a factor of 25. This is a strong indication that the decay model, although useful to understand the decay pattern in general, is inappropriate to identify one critical R, as is common in scale series studies (Heller, 2011). The power curves in Fig. 3 also did not help in identifying a critical R.

Figure 4b shows the ensemble-averaged dimensionless mean vorticity $\omega_m(t)/\Omega_0$ over relative time $t\Omega_0$ for all three scales. A similar pattern in the initial turbulent regime is observed in all three scales whilst the decays deviate in the transition and laminar regime. This is another clear indication of scale effects, which are hoped to be quantified in the near future.

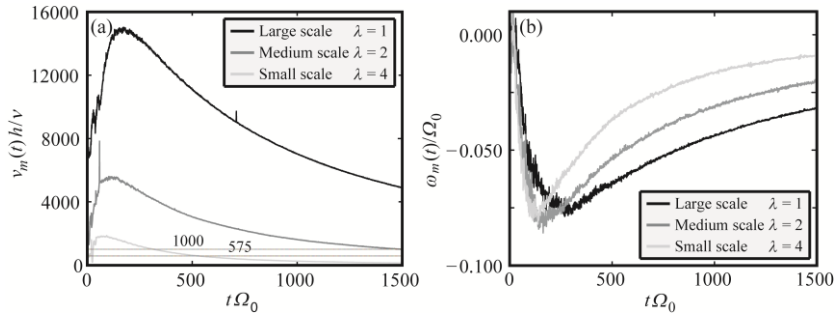


Figure 4: (a) mean Reynolds number $v_m(t)h/\nu$ and (b) dimensionless mean vorticity $\omega_m(t)/\Omega_0$ with relative time $t\Omega_0$.

## 3. Conclusions and outlook

This article highlights the need to investigate scale effects for dissipative-type shallow-water vortices when Reynolds number R invariance can naturally not be maintained. Shallow-water vortices in this context (in absence of Coriolis effects) are relevant in many engineering and small-scale geographical contexts. Results from a laboratory Froude scale series were presented namely the radial-averaged azimuthal velocity over radial distance and the ensemble-averaged mean azimuthal velocity, Reynolds number and dimensionless vorticity decays. These results revealed significant scale effects in the transition and laminar regime. Future work aims (i) to formulate a semi-theoretical model for the time-dependent vortex decay (Figs. 2, 3), (ii) to reveal a critical R to provide clear guidance under which R invariance (negligible R scale effects) applies and (iii) to investigate why some parameters (timing of peaks in Fig. 2, decay rate in Fig. 3) neither follow Froude nor Reynolds scaling. Further physical insight may also be obtained with the help of numerical modelling.

## References


Heller, V. (2011). Scale effects in physical hydraulic engineering models. *J. Hydraul. Res.*, Vol. 49(3), 293-306.

Heller, V. (2017). Self-similarity and Reynolds number invariance in Froude modelling. *J. Hydraul. Res.* (published online).

Jirka, G.H. (2001). Large scale flow structures and mixing processes in shallow flows. *J. Hydraul. Res*., Vol. 39(6), 567-573.

Seol, D.-G., Jirka, G.H. (2010). Quasi-two-dimensional properties of a single shallow-water vortex with high initial Reynolds number. *J. Fluid Mech*., Vol. 665, 274-299.